Mode Completeness, Normalization, and Green's Function of the Inset Dielectric Guide

T. ROZZI, SENIOR MEMBER, IEEE, AND LIZHUANG MA

Abstract — **The inset dielectric guide (IDG) is an easy-to-fabricate alternative to image line that is also less sensitive to loss by radiation at unwanted discontinuities. The discrete spectrum of the IDG was recently analyzed by the transverse resonance diffraction (TRD) method.**

In this paper we complete the characterization of the spectrum to include the continuum. We also address from a fundamental viewpoint the question of its orthonormalization, and determine the Green's function of the guide, which is an essential prerequisite to the analysis of IDG components and of IDG antenna feeds. An application is given to the scattering by a dipole on the air–dielectric interface.

I. INTRODUCTION

CONSIDERABLE EFFORT has been spent on the development of transmission media suitable for microwave and millimeter-wave communications, obvious examples being finline and image line. At high frequencies, as circuit dimensions and tolerances become smaller, the cost of such circuits rises. High circuit costs may in fact become the limiting factor to the ever-increasing commercial development in millimeter-wave technology. Thus, the ease of manufacture and capability for mass production are becoming as important a criterion as the circuit performance of such media.

Image line is a recognized low-loss transmission medium, but its main disadvantage besides manufacturing difficulties is its radiation loss from all practical components. In order to confine the field more to the structure, trapped image guide has been proposed [1], but this is even harder to make, especially for small guide dimensions. In order to overcome such manufacturing difficulties, inset dielectric guide (IDG), shown in cross section in Fig. 1, has been proposed as a low-cost alternative [2]. IDG, which is just a rectangular groove filled with dielectric, has many of the advantages of the trapped image guide without its fabrication problems.

The IDG structure has been analyzed previously, by Zhou and Itoh [3], as an intermediate structure in the analysis of trapped image guide. This analysis used the effective dielectric constant (EDC) method and it gave useful and accurate approximate results for the fundamental mode.

Manuscript received April 17, 1987; revised August 4, 1987. This work was supported in part by British Telecom and the Royal Society.

The authors are with the School of Electrical Engineering, University of Bath, Bath BA2 7AY, United Kingdom.

IEEE Log Number 8718365

The 90° edge, however, imposes a singularity in the transverse fields, which is important for the accurate evaluation of field distributions and radiation properties.

Consideration was given to the above problem in the rigorous, full hybrid treatment in [4] using the method of transverse resonance diffraction (TRD). The discrete spectrum was evaluated, together with propagation losses and Q factors, for the fundamental and a number of higher order discrete modes. Those results show that, away from cutoff, propagation losses are dielectric dominated. Moreover, for practical aspect ratios, assuming a single LSE or LSM potential gives a very good description, provided, that is, the edge conditions are still accounted for in the field distribution assumed over the slot aperture, which implies that the potential is intrinsically nonseparable.

The IDG, however, is an open waveguide and, consequently, its spectrum includes a continuous range of modes. Excitation of the latter takes place due to discontinuities, particularly when these are located close to the air–dielectric interface, such as metal posts (e.g. diodes) or radiating dipoles, if the IDG is to be used as a leaky wave antenna. Therefore, with a view to analyzing practical components in IDG, it is necessary to obtain a complete spectral characterization, inclusive of the continuum. Once the complete spectrum is found, it is possible to construct the appropriate Green's function of the guide for use in the treatment of discontinuity problems. A mathematical difficulty arises at this point inasmuch as the spectral components need to be orthonormalized over the guide cross section.

This trivial task in classical waveguide becomes nontrivial and tedious for guides of inhomogeneous separable cross section, particularly if a continuum is involved.

In the IDG the problem is essentially complicated by the nonseparable nature of the two-dimensional cross section, containing diffraction edges (the metal corners) at the interface between two distinct regions (the slot and the air region). For the one-dimensional separable case (e.g. the multilayer slab), an elegant method based on the transverse equivalent circuit interpretation and the formal properties of the transverse Green's function can be found in textbooks such as [5].

A solution for the two-dimensional, nonseparable, open case such as the IDG has not been reported before.

0018-9480/88/0300-0542$01.00

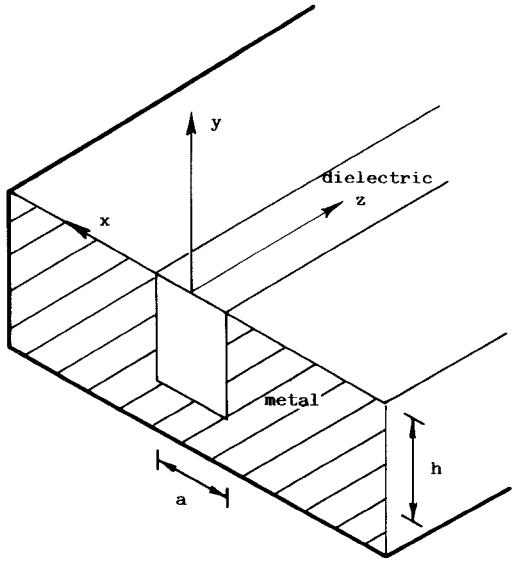

Fig. 1. IDG geometry.

In this paper, it will be shown how the transverse equivalent circuit analogy can be generalized to transverse resonance diffraction and how these concepts can be used to determine the orthonormalized discrete and continuous spectrum of the IDG in the LSE/LSM description.

We will deal first with the question of the normalization of the discrete spectrum in the same representation of the singular field over the slot aperture which was adopted in the TRD solution [4] and then derive the orthonormalized continuum.

The analysis will be developed for the even LSE (TE^Y) polarization, having $E_y = 0$ and E_x as the main electric field component. The scalar Green's function is subsequently obtained and applied to the scattering of a thin transverse dipole at the air–dielectric interface.

II. The Normalized Spectrum of the Slab Waveguide

If the effect of the metal corners of the slot could be ignored, i.e., the side walls were infinitely far removed from each other, the IDG would reduce to a dielectric slab over a ground plane. It is therefore instructive to retrace briefly the procedure involved in determining the normalized complete spectrum of the grounded slab, illustrated in Fig. 2(a). A detailed discussion can be found in [5].

If the expansion of the field takes place in terms of the transverse wavenumber in the air region, k_y, taken as an independent quantity, the wavenumber in the z direction, β, is determined by

$$\beta^2 = k_0^2 - k_y^2. \tag{1}$$

The completeness of the TE spectrum of the slab can then be stated as

$$\sum_s \psi_s(y)\psi_s(y') + \int_0^\infty dk_y \psi(y; k_y)\psi(y'; k_y) \equiv \delta(y - y')$$

where the summation is over the finite number of surface waves, the integral is over the continuum, and the orthonormalization is such that

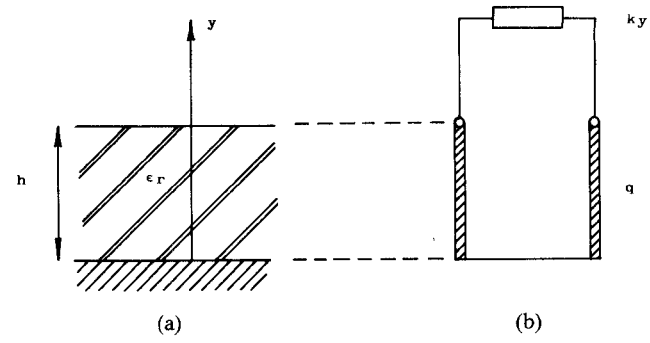

Fig. 2. (a) The metal-backed dielectric slab waveguide and (b) its transverse equivalent circuit.

$$\int_0^\infty dy \psi_s(y)\psi_r(y) = \delta_{sr} \tag{3a}$$

$$\int_0^\infty dy \psi_s(y)\psi(y; k_y) = 0 \tag{3b}$$

$$\int_0^\infty dy \psi(y; k_y)\psi(y; k_y') = \delta(k_y - k_y'). \tag{3c}$$

Analogous expressions hold for the TM case with the weight function $1/\epsilon(y)$.

It is a well-known general property of the Sturm–Liouville equation, in this case the transmission line equation for propagation in the y direction, that the Green's function integrated over a path C in the complex k_y^2 plane to include all singularities yields the delta function. The singularities are constituted by the set of discrete poles corresponding to the discrete spectrum and branch line corresponding to the continuum, namely

$$-\frac{1}{2\pi j}\oint_c g(y, y'; k_y^2)\, dk_y^2 = \delta(y - y'). \tag{4}$$

The Green's function is constructed from two independent solutions of the transverse transmission line equation:

$$\overleftarrow{V} = \frac{\sin q(y + h)}{\sin qh} \tag{5}$$

where

$$\begin{aligned} q^2 &= \epsilon_r k_0^2 - \beta^2 \\ &= k_y^2 + (\epsilon_r - 1)k_0^2 \equiv k_y^2 + v^2 \end{aligned} \tag{6}$$

satisfying the boundary conditions for $y < 0$ and

$$\vec{V} = e^{-jk_y y} \tag{7}$$

satisfying the boundary conditions for $y > 0$ such that $\overleftarrow{V} = \vec{V} = 1$ at $y = 0$.

We have then

$$g = \frac{\overleftarrow{V}(y; k_y^2)\vec{V}(y'; k_y^2)}{j\omega\mu_0 Y(k_y^2)} \tag{8}$$

where Y is the total admittance of the transverse equivalent circuit of Fig. 2(b) (the Wronskian of the transmission line equation, which is independent of position):

$$\omega\mu_0 Y = k_y - jq\cot qh. \tag{9}$$

It is noted for future use that with the above choice of voltage amplitudes, Y represents the complex power of the transverse equivalent circuit.

It can also be seen that the occurrence of a pole of g in the complex k_y^2 plane at $k_y = k_{ys}^2$, say, coincides with the vanishing of the total susceptance of the transverse equivalent network. In order to recover (2) from (4), it is then sufficient to isolate the residues of the poles and modify the integration path so as to go *around* the branch line in the k_y^2 plane, by which process (4) can be rewritten, using (5) and (6), as

$$\sum_s \frac{\overleftarrow{V}(y;k_{ys}^2)\vec{V}(y';k_{ys}^2)}{-j\omega\mu_0 \dfrac{\partial Y}{\partial k_y^2}\Big|_{k_{ys}^2}} + \frac{2}{\pi}\int_0^\infty dk_y\, k_y \mathrm{Im}\frac{\overleftarrow{V}(y;k_y)\vec{V}(y';k_y)}{-j\omega\mu_0 Y(k_y)} \equiv \sum_s \psi_s(y)\psi_s(y') + \int_0^\infty dk_y\, \psi(y;k_y)\psi(y';k_y). \quad (10)$$

In (10), it is then possible to make the identification

$$\psi_s(y) = \frac{\overleftarrow{V}(y;k_{ys}^2)}{\left[-j\omega\mu_0 \dfrac{\partial Y}{\partial k_y^2}\Big|_{k_{ys}^2}\right]^{1/2}}, \qquad y<0 \quad (11)$$

and similarly for $y>0$, yielding the well-known expressions for the TE surface wave of a grounded slab:

$$\psi_s(y) = A_s \frac{\sin q_s(y+h)}{\sin q_s h}, \qquad y \leqslant 0 \quad (12a)$$

$$= A_s e^{-\gamma_s y}, \qquad y \geqslant 0 \quad (12b)$$

with

$$A_s = \sqrt{\frac{2}{h+\dfrac{1}{\gamma_s}}}\sin q_s h, \qquad \gamma_s + q_s \cot q_s h = 0. \quad (13)$$

A substantially analogous procedure leads to the determination of the component of the continuum $\psi(y, k_y)$.

Let us introduce in (9) the following quantity of convenience:

$$\cot\alpha = \frac{q}{k_y}\cot qh \quad (14)$$

and substitute (14) into (8). The resulting expression for a component of the continuum corresponding to the value k_y, $0 \leqslant k_y < \infty$, of the y wavenumber is then

$$\psi(y{:}k_y) = \sqrt{\frac{2}{\pi}}\sin\alpha\frac{\sin q(y+h)}{\sin qh}, \qquad y \leqslant 0 \quad (15a)$$

$$= \sqrt{\frac{2}{\pi}}\sin(k_y y + \alpha), \qquad y \geqslant 0 \quad (15b)$$

which satisfy implicitly the orthonormalization conditions (3). It is noted that the angle α above represents in fact the phase shift a ray with propagation constant (k_y, β) undergoes upon impinging on the slab and reemerging from it.

III. Normalization of the Discrete Spectrum of the IDG

We are now in a position to generalize the previous procedure to the two-dimensional case, such as the IDG. The unnormalized discrete modes were derived in [4] by means of the transverse resonance diffraction method (TRD). We will now proceed to consider the question of their normalization over the guide cross sections in such a manner that

$$\iint_S \phi_s(x,y)\phi_r(x,y)\,dx\,dy = \delta_{sr}. \quad (16)$$

In [4], the distribution at the interface $y=0$ and from there over the whole cross section was derived in terms of the Gegenbauer polynomials [6]

$$\frac{1}{N_m} \qquad C_m^{1/6}\left[\frac{2x}{a}\right]$$

with normalization constant given by

$$N_m^2 = \frac{\pi a 2^{-4/3}\Gamma\left(m+\dfrac{1}{3}\right)}{m!\left(m+\dfrac{1}{6}\right)\Gamma^2\left(\dfrac{1}{6}\right)}$$

orthonormalized in the range $0 \leqslant x \leqslant a/2$ with respect to the weight function

$$W(x) = \left(1-\left(\frac{2x}{a}\right)^2\right)^{-1/3} \quad (17)$$

which implicitly satisfies the edge condition at the 90° corners, thus ensuring rapid convergence. We had, namely, the expression

$$\psi_s(x,0) = W(x)\sum_{m=0}^{2(n-1)} \frac{X_m}{N_m} C_m^{1/6}\left(\frac{2x}{a}\right). \quad (18)$$

The n-dimensional vector $\boldsymbol{X}$ resulted, within an undetermined constant (its norm), from the application of the transverse resonance condition in the form of a diffraction integral (TRD). Owing to the convergence properties of (18), in fact, often just a single term suffices. Now we seek to determine that constant so that the normalization condition (16) is satisfied.

The field at the interface can also be expressed in terms of the discrete Fourier components in the slot as

$$\psi_s(x,0) = \sum_{n=0}^{\infty} E_n \phi_n(x) \quad (19)$$

where

$$\phi_n = \frac{\delta_n}{\sqrt{a}}\cos\frac{n\pi x}{a}, \qquad \delta_n = 2, \quad n>0, \quad \delta_0 = \sqrt{2}$$

and

$$\int_0^{a/2} \phi_m \phi_n\,dx = \delta_{mn}.$$

By orthogonality over the slot, we have

$$E_n = \sum_{m=0}^{N} P_{mn} X_m = \boldsymbol{P}_n^{\tau} \cdot \boldsymbol{X} \tag{20}$$

with

$$P_{mn} = \frac{1}{N_m} \int_0^{a/2} W(x) C_m^{1/6}\left(\frac{2x}{a}\right) \phi_n(x)\, dx$$

$$= \frac{1}{N_m} \frac{\delta_n \sqrt{a}\,(-1)^{m/2} \pi \Gamma\left(m+\frac{1}{3}\right) J_{m+1/6}\left(\frac{n\pi}{2}\right)}{2m!\,\Gamma\left(\frac{1}{6}\right)(n\pi)^{1/6}} \tag{21}$$

as given in [4, eq. (A.6)].

The field anywhere in the slot can therefore be expressed as

$$\psi_s(x, y) = \sum_{n=0}^{\infty} E_n \phi_n(x) \chi_n(y) \tag{22}$$

where

$$\chi_n(y) = \frac{\sin q_n(y+h)}{\sin q_n h}, \qquad q_n^2 = \epsilon_r k_0^2 - \beta^2 - \left(\frac{n\pi}{a}\right)^2.$$

The field at the interface can also be expressed, in terms of the continuous Fourier components in the air region, as

$$\psi_s(x,0) = \int_0^{\infty} dk_x \tilde{E}(k_x) \sqrt{\frac{2}{\pi}} \cos k_x x \tag{23}$$

from which

$$\tilde{E}(k_x) = \boldsymbol{P}^{\tau}(k_x) \cdot \boldsymbol{X}. \tag{24}$$

The components of the vector $\boldsymbol{P}$ are given by

$$P_m(k_x) = \frac{1}{N_m} \int_0^{a/2} W(x) C_m^{1/6}\left(\frac{2x}{a}\right) \sqrt{\frac{2}{\pi}} \cos k_x x\, dx$$

$$= \sqrt{\frac{a}{2\pi}} \frac{1}{\delta_n} P_{mn},$$

$$n = \frac{a k_x}{\pi} \text{ as (21) is valid for any } \textit{real } n. \tag{25}$$

The field anywhere in the air region can then be expressed as

$$\psi_s(x, y) = \int_0^{\infty} dk_x \sqrt{\frac{2}{\pi}} \cos k_x x\, e^{-jk_y y} \boldsymbol{P}^{\tau}(k_x) \cdot \boldsymbol{X}. \tag{26}$$

It is noted explicitly that for a discrete mode, the value $k_{ts}^2 = k_0^2 - \beta_s^2$ is fixed by the transverse resonance condition [4]. As (26) is a Fourier expansion in k_x, taken now as an independent variable, we must choose k_y such that

$$k_{ys} = \sqrt{k_{ts}^2 - k_x^2}, \qquad k_{ts} \geq k_x$$

$$= -j\sqrt{k_x^2 - k_{ts}^2}, \qquad k_x \geq k_{ts}. \tag{27}$$

The amplitudes E_n, $\tilde{E}(k_x)$, X_m can be interpreted as voltages in the equivalent network of Fig. 3, as indicated. This network allows us to write by inspection the total transverse admittance *matrix*, as seen at the reference planes of the interface, in the representation of (18). Looking into the slot region, this is, elementwise,

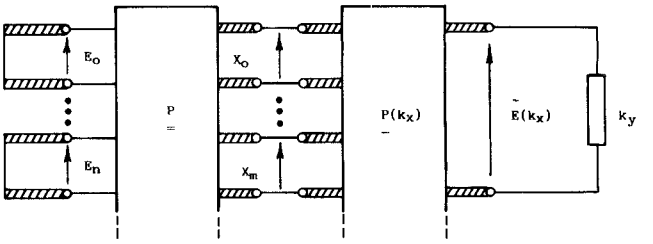

Fig. 3. Transverse equivalent circuit for the normalization of the discrete modes of the IDG.

$$\omega \mu_0 \overleftarrow{Y}_{km} = -j \sum_n q_n \cot q_n h\, P_{kn} P_{mn} \tag{28a}$$

or, in matrix form,

$$\omega \mu_0 \overleftarrow{\boldsymbol{Y}} = -j \sum_n q_n \cot q_n h\, \boldsymbol{P}_n \cdot \boldsymbol{P}_n^{\tau}. \tag{28b}$$

Similarly, looking into the air region,

$$\omega \mu_0 \vec{\boldsymbol{Y}} = \int_0^{\infty} k_y(k_x) \boldsymbol{P}(k_x) \cdot \boldsymbol{P}^{\tau}(k_x)\, dk_x. \tag{29}$$

It is now recalled that the denominator of (8) is just $j\omega\mu_0$ times the complex power for unit voltage at the reference plane $y = 0$ in the one-port situation of Fig. 2(b).

In the multiport situation of Fig. 3, where the voltages at the reference plane are expressed by the vector $\boldsymbol{X}$, the equivalent is given by the scalar

$$p = -j\omega\mu_0 \boldsymbol{X}^{\tau} \cdot \boldsymbol{Y} \cdot \boldsymbol{X} \equiv \omega \mu_0 \boldsymbol{X}^{\tau} \cdot \boldsymbol{B} \cdot \boldsymbol{X} \tag{30}$$

where

$$\boldsymbol{Y} = \overleftarrow{\boldsymbol{Y}} + \vec{\boldsymbol{Y}} = j\boldsymbol{B}.$$

By partial differentiation with respect to k_y^2 at $k_y^2 = k_{ys}^2$, we obtain the actual normalization factor of the discrete modes

$$N_s = \left.\frac{\partial p}{\partial k_y^2}\right|_{k_{ys}^2} = \omega \mu_0 \boldsymbol{X}^{\tau} \cdot \left.\frac{\partial \boldsymbol{B}}{\partial k_y^2}\right|_{k_{ys}^2} \cdot \boldsymbol{X}$$

$$= \frac{1}{2} \boldsymbol{X}^{\tau} \cdot \left[\sum_{n=0}^{\infty} \frac{1}{q_n} \left(q_n h \operatorname{cosec}^2 q_n h - \cot q_n h\right) \boldsymbol{P}_n \boldsymbol{P}_n^{\tau} - j \int_0^{\infty} \frac{dk_x}{k_{ys}} \boldsymbol{P}(k_x) \boldsymbol{P}^{\tau}(k_x) \right] \cdot \boldsymbol{X}. \tag{31}$$

Upon use of (22) and (26), it is straightforward to check by direct quadrature that the above expression just equals

$$N_s = \sum_n E_n^2 \frac{\partial}{\partial k_y^2}(-q_n \cot q_n h) + \int_0^{\infty} dx_k \tilde{E}^2(k_x) \frac{\partial}{\partial k_y^2}(-jk_y) =$$

$$= \iint_S \psi_S^2(x, y)\, dx\, dy \tag{32}$$

where it is noted that the derivative of the susceptance for the nth or k_x Fourier component is in fact identical to the integral of the square of the y dependence.

In conclusion, if the as yet unspecified norm of $\boldsymbol{X}$ is chosen so that $N_s = 1$ in (31), the orthonormalized distribution of the discrete mode is given by (22) for $y \leqslant 0$ and by (26) for $y \geqslant 0$.

IV. Determination of the Orthonormalized Continuous Spectrum of the IDG

Unlike the discrete spectrum, derived previously in [4] within a normalization constant N_s, which could always be determined, albeit laboriously, by direct integration, the continuum was not reported before. It constitutes, in fact, an example of a two-dimensional, nonseparable problem which cannot be reduced to a uniform spectral-domain description because of the change of cross section at the interface.

As the cross section is two-dimensional, it is apparent that an expansion of the continuum can be written in terms of two independent wavenumbers, the third being fixed by the wave equation. We choose $(k_x, k_y) = \boldsymbol{k}_t$ as the two independent quantities and, correspondingly, develop the field in the air region in terms of partial waves of the type

$$\sqrt{\frac{2}{\pi}} \cos k_x x \sqrt{\frac{2}{\pi}} \sin(k_y y + \alpha) \tag{33}$$

which highlights the correspondence with the slab case as $k_x \to 0$. It is noted, however, that the "phase shift" α is now a function of both k_x and k_y because of the nonseparability caused by the presence of the corners.

It is noted that the transverse Green's admittance function (8) only contains $k_y^2(k_x^2)$; hence k_x, k_y can be limited to the interval $0 \leqslant k_x,\ k_y < \infty$. Physically, this is a consequence of choosing to represent the continuum by a set of standing waves.

We require that the components of the continuum satisfy the orthogonality conditions:

$$\begin{aligned}\iint_S \psi(x, y; k_x, k_y)\psi(x, y: k_x', k_y')\, dx\, dy &= \delta(k_x - k_x')\cdot\delta(k_y - k_y') \\ &\equiv \delta(\boldsymbol{k}_t - \boldsymbol{k}_t').\end{aligned} \tag{34}$$

In the treatment of the discrete spectrum, we found it convenient to expand the field at the interface in terms of discrete basis functions individually satisfying the edge conditions at the metal corners. This is not required of individual components of the continuum, but only of the total field. Therefore in consideration of the partial wave expression (33) we now find it convenient to expand the field at the interface directly in terms of the x dependence of the partial waves, i.e., a continuum in k_x. This fact imposes a generalization to the concept of the discrete transverse admittance matrix $\boldsymbol{Y}$ we met in the previous section as follows.

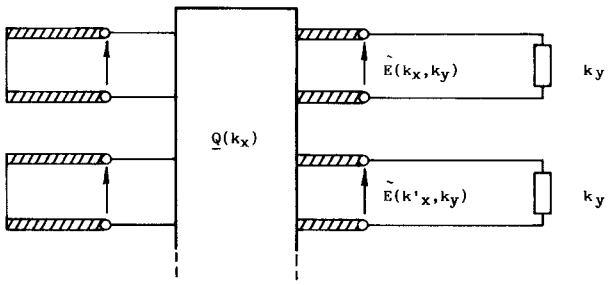

Fig 4. Transverse equivalent circuit for deriving the orthonormalized continuum of the IDG.

The transverse equivalent circuit appropriate to the new situation is shown in Fig. 4. The discontinuous interface acts as an ideal transformer coupling slot components with a different wavenumber $n\pi/a$ and partial waves in air with different wavenumber k_x.

We shall now generalize to two dimensions the method described in Section II, eq. (10). This involves constructing the Green's function from an outward and an inward-traveling wave at the interface $y = 0$.

An outward-traveling partial wave in the air region with wavenumber $\boldsymbol{k}_t$ and Fourier amplitude $\tilde{E}(\boldsymbol{k}_t)$ is expressed as

$$\vec{V}(x, y; \boldsymbol{k}_t) = \sqrt{\frac{2}{\pi}}\, \tilde{E}(\boldsymbol{k}_t) \cos k_x x\, e^{-jk_y y}. \tag{35}$$

Correspondingly, there exists a standing wave in the slot expressible as

$$\overleftarrow{V}(x, y; \boldsymbol{k}_t) = \sum_{n = 0,2,\cdots}^{\infty} Q_n(k_x)\phi_n(x)\chi_n(y). \tag{36}$$

The scalar continuity condition is replaced by

$$\overleftarrow{V}(x,0; \boldsymbol{k}_t) = \vec{V}(x,0; \boldsymbol{k}_t) \tag{37}$$

which allows the coefficients Q_n in (36) to be determined by orthogonality of the ϕ_n's over the slot:

$$Q_n(k_x) = \sqrt{\frac{2}{\pi a}}\, \delta_n (-1)^{n/2} \cdot \sin\frac{k_x a}{2} \frac{k_x}{k_x^2 - \left(\frac{n\pi}{a}\right)^2} \tilde{E}(\boldsymbol{k}_t). \tag{38}$$

Also, from the equivalent circuit of Fig. 4, the susceptance looking into the slot, as seen from reference planes at $y = 0^+$, is given by the parallel combination of the transverse transmission lines, corresponding to the various values of n in the slot. These lines are terminated by a short circuit at $y = -h$, as seen via the transformer Q, namely

$$\omega\mu_0 \overleftarrow{B}(k_x, k_x') = -\sum_n q_n \cot q_n h\, Q_n(k_x) Q_n(k_x'). \tag{39}$$

In the air region, the two different components k_x and k_x' do not couple and a component with y-directed wavenumber k_y propagates in the positive y direction with a characteristic admittance $k_y/\omega\mu_0$. These facts imply that the admittance is a delta function of k_x with amplitude

k_y, namely

$$\omega\mu_0\vec{B}(k_x, k_x') = \frac{1}{j}k_y\delta(k_x - k_x'). \tag{40}$$

Let $B(k, k_x') = \overleftarrow{B} + \vec{B}$. If $\tilde{E}(\boldsymbol{k}_t)$ is set equal to unity in (35), the complex power (times $-j\omega\mu_0$) corresponding to the components $\boldsymbol{k}_t = (k_x, k_y)$ is then given by

$$p(\boldsymbol{k}_t) = \omega\mu_0\tilde{E}(\boldsymbol{k}_t)\int_0^\infty B(k_x, k_x')\tilde{E}(k_x', k_y)\,dk_x'$$
$$= \omega\mu_0\int_0^\infty B(k_x, k_x')\,dk_x'. \tag{41}$$

Hence, from (39) and (40)

$$p = \frac{1}{j}k_y - \sum_n q_n \cot q_n h \sqrt{\frac{\pi}{2a}}\,\delta_n Q_n(k_x) \tag{42}$$

as

$$\int_0^\infty Q_n(k_x)\,dk_x = \sqrt{\frac{\pi}{2a}}\,\delta_n.$$

It is again useful to define a quantity of convenience $\alpha(k_x, k_y)$ such that

$$\cot\alpha = \frac{1}{k_y}\sum_n q_n \cot q_n h \sqrt{\frac{\pi}{2a}}\,\delta_n Q_n(k_x). \tag{43}$$

Using (43) in (8), we have then

$$\frac{2}{\pi}k_y \mathrm{Re}\left[\frac{\overleftarrow{V}\vec{V}}{k_y - jk_y\cot\alpha}\right] = \sqrt{\frac{2}{\pi}}\sum_n Q_n\phi_n(x)\chi_n(y)\sin\alpha$$
$$\cdot\frac{2}{\pi}\cos k_x x' \sin(k_y y' + \alpha)$$
$$\equiv \psi(x, y; \boldsymbol{k}_t)\psi(x', y'; \boldsymbol{k}_t)$$

from which the components of the continuum can be identified as

$$\psi(x, y; \boldsymbol{k}_t) = \sqrt{\frac{2}{\pi}}\sin\alpha(\boldsymbol{k}_t)$$
$$\cdot\sum_n Q_n(k_x)\phi_n(x)\chi_n(y), \qquad y \leqslant 0$$
$$= \frac{2}{\pi}\cos k_x x \sin(k_y y + \alpha), \qquad y \geqslant 0. \tag{45}$$

It can be checked by direct integration that the orthonormalization condition (34) over the cross section is indeed satisfied by (45) (see the Appendix).

V. The Green's Function of the IDG

Having constructed the complete, orthonormalized spectrum of the IDG for E^x polarization, we are now in a position to formulate its scalar Green's function. The latter is a prerequisite for the solution of discontinuity problems.

The scalar Green's function $G(\boldsymbol{r}, \boldsymbol{r}')$ is the solution of the inhomogeneous wave equation with a delta function source located at $\boldsymbol{r}'$, namely

$$\nabla^2 G + \epsilon_r k_0^2 G = \delta(\boldsymbol{r} - \boldsymbol{r}') \tag{46}$$

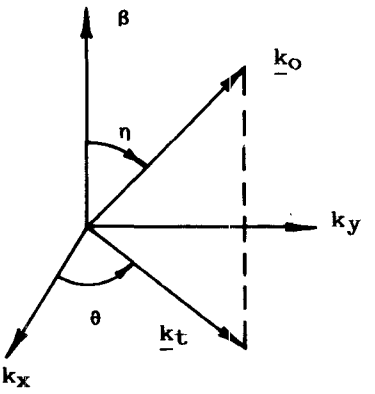

Fig. 5. Trigonometric decomposition of the wavenumber.

with the boundary conditions appropriate to E_x. This should not be confused with the two-dimensional g used in Section II, which refers to the transverse wave equation, in the process of determining the spectrum of the guide.

Inasmuch as the normalized mode spectrum is now known, the Green's function solution of (46) is found by the classical method of expansion in eigenmodes [7], right and left of the source function ($z \leqslant z'$ and $z \geqslant z'$).

By imposing the continuity of G at the source point $z = z'$ and by the condition that its derivative be discontinuous there by the unit step, we recover the classical expression for the eigenmode expansion of the Green's function valid at each side of the source point:

$$G(\boldsymbol{r}, \boldsymbol{r}') = \sum_s \frac{1}{2j\beta_s}\psi_s(x, y)\psi_s(x', y')e^{-j\beta_s|z - z'|} \tag{47}$$

the summation being over the spectrum. Referring, in particular, to a guide with a single bound mode and making explicit the contribution of the continuum, (47) can be rewritten as

$$G(\boldsymbol{r}, \boldsymbol{r}') = \frac{1}{2j\beta_s}\psi_s(x, y')\psi_s(x', y')e^{-j\beta_s|z - z'|}$$
$$+ \int_0^\infty dk_x \int_0^\infty dk_y \frac{e^{-j\beta|z - z'|}}{2j\beta}$$
$$\cdot\psi(x, y; \boldsymbol{k}_t)\psi(x', y'; \boldsymbol{k}_t) \tag{48}$$

where $\beta = \sqrt{k_0^2 - k_t^2}$.

The evaluation of the double integral in the wavenumber space is conveniently carried out by trigonometric transformations, as illustrated in Fig. 5. These are

$$\beta = k_0\cos\eta \tag{49a}$$
$$k_t = k_0\sin\eta \tag{49b}$$
$$k_x = k_t\cos\theta \tag{49c}$$
$$k_y = k_t\sin\theta. \tag{49d}$$

Owing to (49), we have

$$\frac{dk_x\,dk_y}{\beta} = \frac{k_t\,dk_t\,d\theta}{\beta} = k_t\,d\eta\,d\theta.$$

Regarding the path of integration in the η and θ planes, inasmuch as we have chosen expansions in terms of k_x, k_y

real and such that $0 \leqslant k_x,\ k_y < \infty$, θ is a real angle:

$$0 \leqslant \theta \leqslant \frac{\pi}{2}.$$

The integration in the complex η plane, however, runs over the real interval

$$0 \leqslant \operatorname{Re}\eta \leqslant \frac{\pi}{2} \qquad \operatorname{Im}\eta = 0$$

and then over the imaginary interval

$$\operatorname{Re}\eta = \frac{\pi}{2} \qquad 0 \leqslant \operatorname{Im}\eta < \infty.$$

If the nonradiative continuum corresponding to $k_t > k_0$ is neglected, then so is the contribution of the latter interval and η is a real angle

$$0 \leqslant \eta \leqslant \frac{\pi}{2}.$$

The above trigonometric transformation is in fact a preliminary to the evaluation of the far field radiated by a dipole.

VI. Scattering by a Small, Thin Transverse Dipole on the Air–Dielectric Interface

The transverse electric field at the air–dielectric interface $y = 0$ is near its maximum value. The interface also constitutes the most accessible plane of the guide. This is therefore an ideal location for a source, such as a diode, placed across the slot aperture or for a discontinuity, such as a metal strip or disk, with a view to realizing circuit elements or a leaky wave antenna. As an example of the application of the Green's function (48), we shall therefore consider the scattering by a small, thin transverse current element, representing an independent source of an induced one, located at $z = 0$, sufficiently thin and small to be representable as

$$J(x,z) = J_0\delta(z), \qquad 0 \leqslant |x| < \frac{l}{2}$$
$$= 0, \qquad \frac{l}{2} \leqslant |x| \tag{50}$$

with constant J_0. The scalar Green's function (48) is that pertaining to an x-directed electric field distribution assumed as the source of the EM field. If the source term is constituted by an x-directed electric current J, then the electric field E_x is related to G through the x component of the vector potential A, given by

$$A_x(\boldsymbol{r}) = -\mu_0 \int_{-l/2}^{+l/2} G(\boldsymbol{r}; x', 0, 0) J(x')\, dx' \tag{51}$$

and the resulting scattered field is

$$E_x^s = -j\omega A_x + \frac{1}{j\omega\mu_0\epsilon_0}\frac{\partial^2}{\partial x^2}A_x \tag{52}$$

$$= j\omega\mu_0 \int_{-l/2}^{+l/2} \left(1 + \frac{1}{k_0^2}\frac{\partial^2}{\partial x^2}\right) GJ(x')\, dx' \tag{53}$$

$$= \frac{\omega\mu_0}{2} J_0 \left(\frac{\tilde{\psi}_s(x,y)}{\beta_s} D_s e^{-j\beta_s|z|} + \int_0^{\pi/2} d\eta \int_0^{\pi/2} d\theta\, k_0 \sin\eta \cdot \tilde{\psi}(x,y;\eta,\theta) D(\eta,\theta) e^{-jk_0\cos\eta|z|} \right)$$

where

$$\tilde{\psi}_s = \left(1 + \frac{1}{k_0^2}\frac{\partial^2}{\partial x^2}\right)\psi_s \tag{54a}$$

$$\tilde{\psi}(x,y,\eta,\theta) = \left[1 + \frac{1}{k_0^2}\frac{\partial^2}{\partial x^2}\right]\psi(x,y,\eta,\theta) \tag{54b}$$

which can be evaluated directly from (22), (26), and (45) accordingly as $y < 0$ (slot region) or $y > 0$.

In (53) we have

$$D_s = 2\int_0^{l/2} \psi_s(x',0)\, dx' \approx \frac{X_0}{N_0} l \left[1 + \left(\frac{l}{3a}\right)^2\right] \tag{55}$$

using the expansion (18) with a single term, and

$$D(\eta,\theta) = 2\int_0^{l/2} \psi(x',0;\eta,\theta)\, dx'$$
$$= \frac{4}{\pi}\sin\alpha(\eta,\theta)\frac{\sin\left(\sin\eta\cos\theta\dfrac{k_0 l}{2}\right)}{k_0\sin\eta\cos\theta} \tag{56}$$

where

$$\cot\alpha = \frac{1}{k_0\sin\eta\sin\theta}\sum_{n=0,2,}^{\infty}\sqrt{\frac{\pi}{2a}}\,\delta_n Q_n q_n \cot q_n h \tag{57a}$$

$$q_n^2 = v^2 - \left(\frac{n\pi}{a}\right)^2 + k_0^2\sin^2\eta \tag{57b}$$

$$Q_n = \sqrt{\frac{2}{a\pi}}\,\delta_n(-1)^{n/2}\sin\left(\sin\eta\cos\theta\frac{k_0 a}{2}\right) \cdot \frac{\sin\eta\cos\theta\, k_0}{(k_0\sin\eta\cos\theta)^2 - \left(\dfrac{n\pi}{a}\right)^2}.$$

In spite of its apparent complexity, the double integral (53) is in fact amenable to straightforward numerical integration. Moreover, the trigonometric form of the integrand lends itself naturally to the evaluation of the far field by the saddle point method.

VII. Far-Field Pattern of the Dipole: Excitation of the Fundamental Mode

The evaluation of the far field is effected by going over to cylindrical coordinates in the radiation integral in (53), as shown in Fig. 6:

$$x = R\cos w$$
$$y = R\sin w$$

so that

$$k_x x + k_y y = k_0 R\sin\eta\cos(\theta - w). \tag{58}$$

Upon using the symmetry of the integrand with respect to θ, the radiation integral in (53) can be rewritten as

$$E_x^s = \frac{j\omega\mu_0}{4\pi} J_0 \int_0^{\pi/2} d\eta \int_{-\pi/2}^{\pi/2} d\theta\, k_0 \sin\eta \cdot \left(1 - \sin^2\eta\cos^2\theta\right) D(\eta,\theta) \cdot e^{-j\alpha} \cdot e^{-jk_0 R\sin\eta\cos(\theta - w)}. \tag{59}$$

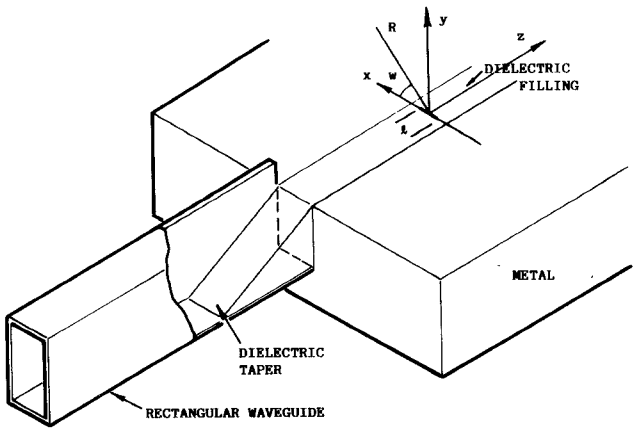

Fig. 6. Transverse dipole on IDG, showing transition from rectangular waveguide.

There is no pole in the integrand, so that when $k_0R \gg 1$, by using the saddle point method we obtain

$$E_x^s \approx -\frac{\omega\mu_0 J}{2R}\sin^2 w\, D\left(\frac{\pi}{2}, w\right) e^{-j\alpha(\pi/2, w)} e^{-jk_0R}. \quad (60)$$

The radiation pattern is then given by

$$f(w) = \left|\frac{E_x^s(w)}{E_x^s\left(\frac{\pi}{2}\right)}\right|^2 = \sin^4 w \left|\frac{D\left(\frac{\pi}{2}, w\right)}{D\left(\frac{\pi}{2}, \frac{\pi}{2}\right)}\right|^2. \quad (61)$$

From (56) and (57) we deduce

$$D\left(\frac{\pi}{2}, w\right) = \frac{4}{\pi}\sin\alpha\left(\frac{\pi}{2}, w\right)\frac{\sin\left(\frac{k_0 l}{2}\cos w\right)}{k_0 \cos w} \quad (62a)$$

$$D\left(\frac{\pi}{2}, \frac{\pi}{2}\right) = \frac{2l}{\pi}. \quad (62b)$$

Hence, the resulting radiation pattern is

$$f(w) = \left(\frac{\pi}{2l}\sin^2 w D\left(\frac{\pi}{2}, w\right)\right)^2 \quad (63)$$

showing the influence of the IDG geometry on the radiation pattern while $\sin^2 w$ represents the usual pattern of a dipole in an infinite space.

The radiation pattern is plotted in Fig. 7 for various values of $k_0 l, l/a$, and is compared with that of an isolated dipole in free space, namely, $\sin^2 w$. It is apparent from the figure that the effect of the inset guide backing of the dipole is to narrow considerably the radiation pattern, as a result of the presence of the ground plane. Moreover, the pattern is only weakly dependent on the frequency, as the latter only affects $f(w)$ via α and the ratio in (62a).

The dipole also excites a forward- and a backward-traveling wave in the fundamental mode, whose amplitude is determined by multiplying (53) by ψ_s and integrating over S. This is

$$A_s^+ = A_s^- \simeq \frac{\omega\mu_0}{2} J_0 \frac{D_s}{\beta_s}\iint_S \psi_s \psi_s\, dx\, dy = \frac{\omega\mu_0}{2} J_0 \frac{D_s}{\beta_s} \quad (64)$$

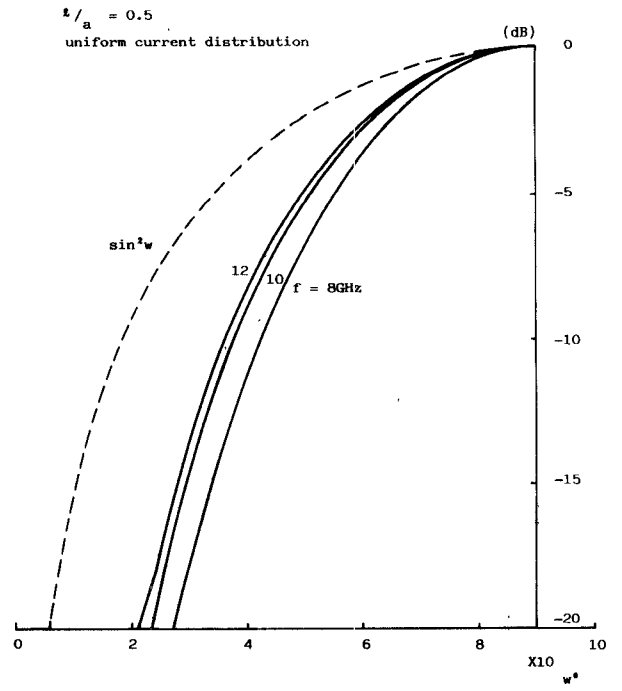

(a)

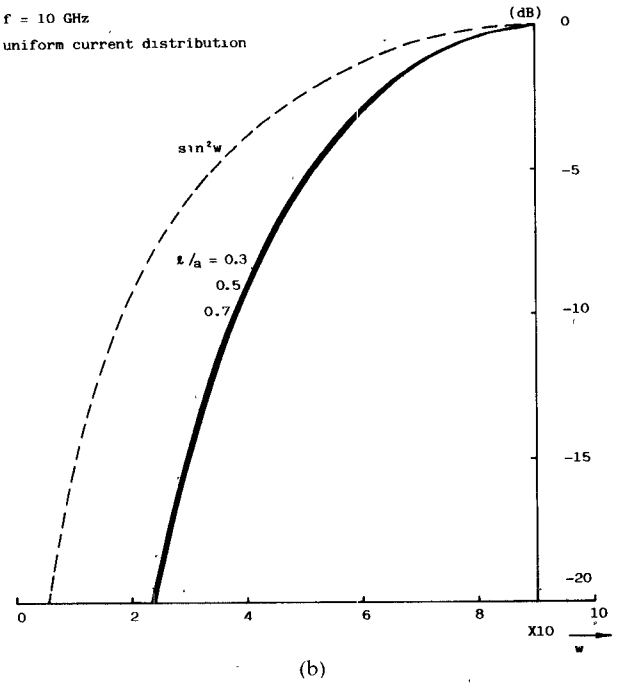

(b)

Fig. 7. Far field pattern for the dipole of Fig. 6.

where we have neglected weak "overlapping" terms of ψ_s with $\tilde{\psi}$ (radiation resistance) and $\partial^2/\partial x^2 \psi_s$ (coupling different Fourier components in the slot).

In the above, J_0 may be the amplitude of an independent source, say a diode, or that of an induced one, say the current induced on a metal strip by the fundamental mode ψ_s itself, incident with unit amplitude. In the latter case, J_0 is determined rigorously by the condition that the total field on the metal strip vanish.

Within the scope of small dipole approximation adopted in this section $J_0 \approx H_{zs}$ and again neglecting second de-

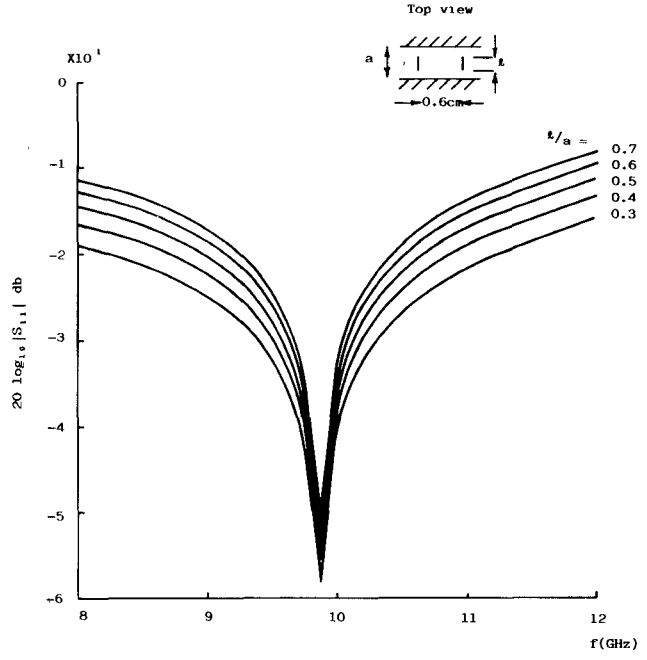

Fig. 8. Reflection and transmission coefficient of small dipole.

rivatives with respect of x, i.e., by assuming the propagating mode to be pure TE rather than LSE and separable, and only retaining the contribution of the slot region, we further obtain

$$J_0 \approx \frac{1}{\omega\mu_0}\sum_n q_n \cot q_n h\, P_{0n}^2. \tag{65}$$

Hence by substituting the above approximate amplitude in (64), we can identify A_s^- with the reflection coefficient Γ of the metal strip, i.e.,

$$\Gamma = A_s^- \cong \frac{\Sigma q_n \cot q_n h\, P_{0n}^2}{2\beta_s} l\left(1+\left(\frac{l}{3a}\right)^2\right) \tag{66}$$

which is valid for thin strips $l/a < 1$. When two identical dipoles are located a quarter wavelength apart, cancellation of the overall reflection coefficient occurs. This effect is illustrated in Fig. 8, showing the magnitude of the reflection coefficient versus frequency for various dipole lengths, computed from (66) by elementary network analysis. The spacing between the two dipoles (0.6 cm) is such that $f_0 = 9.875$ GHz corresponds to a quarter wavelength in the guide.

VII. Conclusions

We have derived the complete orthonormalized spectrum of the IDG from basic principles as an original example of a nonseparable two-dimensional problem involving both a closed region, an open region and diffracting corners.

In particular, the discrete modes are expressed in terms of suitable functions at the air–dielectric interface, individually satisfying the edge conditions, whereas the continuous modes are expressed conveniently in terms of partial waves in the air region. The Green's function of the guide is then derived in terms of the complete spectrum, a step that is prerequisite to the rigorous solution of discontinuity and radiation problems in IDG. An application is given to the scattering by a small transverse dipole placed at the air–dielectric interface, obtaining analytically the far field and quasi-analytically the near field.

Appendix
Direct Check on Orthonormality of the Continuum

We want to verify that the condition

$$\iint_S dx\,dy\,\psi(x,y;\boldsymbol{k}_t)\psi(x,y;\boldsymbol{k}_t) = \delta(\boldsymbol{k}_t - \boldsymbol{k}_t') \tag{A1}$$

is satisfied by direct integration. Define by I_1 the integral over the slot cross section. This is given by

$$I_1 = \int_0^{a/2} dx \int_{-h}^{0} dy \sum_n Q_n(k_x)Q_n(k_x')\sin\alpha\sin\alpha' \cdot \phi_n(x)\phi_n'(x)\frac{2}{\pi}\frac{\sin q_n(y+h)}{\sin q_n h}\cdot\frac{\sin q_n'(y+h)}{\sin q_n' h} \tag{A.2}$$

where

$$\alpha' = \alpha(k_x', k_y') \qquad q_n^2 = (\epsilon_r - 1)k_0^2 - k_t^2 - \left(\frac{n\pi}{a}\right)^2.$$

By orthogonality of the ϕ_n and integration over y, we have

$$\begin{aligned} I_1 &= \sum_n Q_n(k_x)Q_n(k_x')\cdot\frac{\sin\alpha}{\sin q_n h}\cdot\frac{\sin\alpha}{\sin q_n' h}\cdot\frac{1}{\pi} \\ &\quad\cdot\left[\frac{\sin(q_n - q_n')h}{q_n - q_n'} - \frac{\sin(q_n + q_n')h}{q_n + q_n'}\right] \\ &= \frac{2}{\pi}\frac{\sin\alpha\sin\alpha'}{k_t^2 - k_t'^2}\sum_n Q_n(k_x)Q_n(k_x') \\ &\quad\cdot(q_n'\cot q_n' h - q_n\cot q_n h). \end{aligned}$$

In the air region, we have

$$\begin{aligned} I_2 &= \int_0^\infty dx\int_0^\infty dy\,\frac{2}{\pi}\cos k_x x\cos k_x' x \\ &\quad\cdot\frac{2}{\pi}\sin(k_y y+\alpha)\sin(k_y' y+\alpha') \\ &= \delta(k_x - k_x')\left\{\delta(k_y - k_y') - \frac{1}{\pi}\right. \\ &\qquad\left.\cdot\left[\frac{\sin(\alpha-\alpha')}{k_y - k_y'} - \frac{\sin(\alpha+\alpha')}{k_y + k_y'}\right]\right\} \\ &= \delta(k_x - k_x')\left\{\delta(k_y - k_y') - \frac{2}{\pi}\frac{\sin\alpha\sin\alpha'}{k_y^2 - k_y'^2}\right. \\ &\qquad\left.\cdot(k_y'\cot\alpha' - k_y\cot\alpha)\right\}. \end{aligned}$$

Satisfaction of (A1) implies

$$I_1 + I_2 = \delta(k_x - k_x')\,\delta(k_y - k_y'). \tag{A5}$$

If the second term in (A4) equals I_1, this is indeed the case. It is now verifiable that (A5) holds provided α is chosen such that

$$k_y \cot \alpha \delta(k_x - k_x') = \sum_n Q_n(k_x) Q_n(k_x') q_n \cot q_n h. \quad \text{(A6)}$$

Integrating w.r.t. k_x' from 0 to ∞, we recover

$$k_y \cot \alpha = \sum_n \sqrt{\frac{\pi}{2a}}\, \delta_n Q_n(k_x) q_n \cot q_n h \quad \text{(A7)}$$

which is just our definition (43) of α.

REFERENCES

[1] T. Itoh and B. Adelseck, "Trapped image guide for millimetre wave circuits," *IEEE Trans. Microwave Theory Tech.*, vol. MTT-28, pp. 1433–1436, Dec. 1980.

[2] S. C. Gratze, "Inset dielectric waveguide," Proposal YBO 881, Marconi Research Laboratories.

[3] W. Zhou and T. Itoh, "Analysis of trapped image guides using effective dielectric constant and surface impedances," *IEEE Trans. Microwave Theory Tech.*, vol. MTT-30, pp. 2163–2166, Dec. 1982.

[4] T. Rozzi and S. Hedges, "Rigorous analysis and network modelling of inset dielectric guide," presented at 15th European Microwave Conf., Paris, September 1985; to appear in *IEEE Trans. Microwave Theory Tech.*

[5] L. Felsen and N. Marcuvitz, *Radiation and Scattering of Waves*. Englewood Cliffs, NJ: Prentice Hall, 1973, ch. 3, pp. 278–282.

[6] I. S. Gradshteyn and I. Rizhik, *Tables of Series and Integrals*, New York: Academic Press, 1965, p. 827.

[7] R. Collin, *Field Theory of Guided Waves*. New York: McGraw-Hill, 1964, ch. 7, pp. 262–264.

T. Rozzi (M'66–SM'74) obtained the degree of 'Dottore' in physics from the University of Pisa in 1965 and the Ph.D. degree in electronic engineering at Leeds University in 1968. In June 1987 he received the degree of D.Sc from the University of Bath.

From 1968 to 1978 he was a Research Scientist at the Philips Research Laboratories, Eindhoven, the Netherlands, having spent one year, 1975, at the Antenna Laboratory, University of Illinois, Urbana. In 1975 he was awarded the Microwave Prize of the Microwave Theory and Technique Group of the Institute of Electrical and Electronic Engineers. In 1978 he was appointed to the Chair of Electrical Engineering at the University of Liverpool and subsequently was appointed to the Chair of Electronics and Head of the Electronics Group at the University of Bath in 1981. From 1983 to 1986 he held the additional responsibility of Head of the School of Electrical Engineering at Bath. In 1986 Dr. Rozzi was called to the 'ordinary chair' of Antennas at the Faculty of Engineering, University of Ancona, Italy.

✠

Lizhuang Ma was born on February 19, 1945, in Peking, China. She graduated from the Department of Radio-Electronics, Tsinghua University, in March 1970. From 1970 to 1984 she taught and conducted research in that department. In the academic year 1984–85 she was a Visiting Scholar at the School of Electrical Engineering, University of Bath, U.K. Currently she is a Research Officer at the school Her current interests are in the transverse resonance diffraction analysis of dielectric transmission lines and the design of integrated millimeter-wave antennas.